Robustness of solar neutrino oscillations in the presence of non–standard physics[1]

O. G. Miranda*, M. A. Tórtola† and J. W. F. Valle**

*Departamento de Física, Centro de Investigación y de Estudios Avanzados del IPN
Apdo. Postal 14-740 07000 Mexico, DF, Mexico.
†Centro de Fíisica Teórica de Partículas. Departamento de Física. Instituto Superior Técnico.
Avenida Rovisco Pais, 1049-001 Lisboa, Portugal.
**AHEP Group, Instituto de Física Corpuscular – C.S.I.C./Universitat de València
Edificio Institutos de Paterna, Apt. 22085, E–46071 València, Spain

Abstract. We have reconsidered the status of the large mixing angle (LMA) oscillation interpretation of the solar neutrino data in a more general framework where non-standard neutrino interactions are present. Using the latest data from all solar neutrino experiments and KamLAND we have found the existence of three LMA solutions, instead of the unique solution which holds in the absence of non-standard interactions, LMA-I. In addition to LMA-I, there is another solution with smaller value of Δm^2 (LMA-0), and a new "dark-side" solution (LMA-D) with $\sin^2\theta = 0.70$. We comment on the complementary role of atmospheric, laboratory, reactor and future solar neutrino experiments in lifting the degeneracy between this three solutions. We also mention that establishing the issue of robustness of the oscillation picture in the most general case will require further experiments, such as those involving low energy solar neutrinos.

Keywords: Neutrino masses and mixings, Solar neutrinos, Neutrino interactions
PACS: 14.60.Pq, 13.15.+g

INTRODUCTION

The first data of the KamLAND collaboration [2] have been enough to isolate neutrino oscillations as the correct mechanism explaining the solar neutrino problem, indicating also that large mixing angle (LMA) was the right solution. The 766.3 ton-yr KamLAND data sample strengthens the validity of the LMA oscillation interpretation of the data [3]. With neutrino experiments now entering the precision age [4], the determination of neutrino parameters and their theoretical impact have become one of the main goals in astroparticle and high energy physics [5]. Now the main efforts should be devoted to the precision determination of the oscillation parameters and to test for sub-leading non-oscillation effects such as spin-flavour conversions [6, 7] or non-standard neutrino interactions (NSI) [8].

Here we focus on the case of neutrinos endowed with non-standard interactions. These are a natural outcome of many neutrino mass models [9] and can be of two types: flavour-changing (FC) and non-universal (NU). Non–standard interactions may in principle affect neutrino propagation properties in matter as well as detection cross sections. Thus their existence can modify the solar neutrino signal observed at experiments. They may

[1] Based on the results of Ref. [1]

CP917, *Particles and Fields,* edited by H. Castilla Valdez, J. C. D'Olivo, and M. A. Perez

be parametrized with the effective low–energy four–fermion operator:

$$\mathscr{L}_{NSI} = -\varepsilon_{\alpha\beta}^{fP} 2\sqrt{2} G_F \left(\bar{\nu}_\alpha \gamma_\mu L \nu_\beta\right) \left(\bar{f} \gamma^\mu P f\right), \tag{1}$$

where P = L, R and f is a first generation fermion: e, u, d. The coefficients $\varepsilon_{\alpha\beta}^{fP}$ denote the strength of the NSI between the neutrinos of flavours α and β and the P–handed component of the fermion f. In the present work, for definiteness, we take for f the down-type quark. However, one can also consider the presence of NSI with electrons and up and down quarks simultaneously. Current limits and perspectives in the case of NSI with electrons have been reported in the literature [10]. While strong constraints exist from ν_μ interactions with a down-type quark ($\varepsilon_{e\mu}^{dP} \lesssim 10^{-3}$, $\varepsilon_{\mu\mu}^{dP} \lesssim 10^{-3} - 10^{-2}$) from CHARM and NuTeV [11], the constraints for all other NSI couplings, including those involved in solar neutrino physics, are rather loose [11, 12]. Therefore, in our analysis we consider $\varepsilon_{\alpha\mu}^{dP} = 0$ and we concentrate our efforts in the rest of NSI parameters.

For our solar neutrino analysis, we will consider the simplest approximate two–neutrino picture, which is justified in view of the stringent limits on θ_{13} [5] that follow mainly from reactor neutrino experiments [13]. In this approximation, the Hamiltonian describing solar neutrino evolution in the presence of NSI contains, in addition to the standard oscillations term

$$\begin{pmatrix} -\frac{\Delta m^2}{4E}\cos 2\theta + \sqrt{2}\,G_F N_e & \frac{\Delta m^2}{4E}\sin 2\theta \\ \frac{\Delta m^2}{4E}\sin 2\theta & \frac{\Delta m^2}{4E}\cos 2\theta \end{pmatrix} \tag{2}$$

a term $H_{\rm NSI}$, accounting for an effective potential induced by the NSI with matter, which may be written as:

$$H_{\rm NSI} = \sqrt{2} G_F N_d \begin{pmatrix} 0 & \varepsilon \\ \varepsilon & \varepsilon' \end{pmatrix}. \tag{3}$$

Here ε and ε' are two effective parameters that, according to the current bounds discussed above ($\varepsilon_{\alpha\mu}^{fP} \sim 0$), are related with the fundamental couplings of Eq. (1) by:

$$\varepsilon = -\sin\theta_{23}\,\varepsilon_{e\tau}^{dV} \qquad \varepsilon' = \sin^2\theta_{23}\,\varepsilon_{\tau\tau}^{dV} - \varepsilon_{ee}^{dV} \tag{4}$$

The quantity N_d in Eq. (3) is the number density of the down-type quark along the neutrino path. It is important to note that the neutrino evolution inside the Sun and the Earth is sensitive only to the vector component of the NSI, $\varepsilon_{\alpha\beta}^{dV} = \varepsilon_{\alpha\beta}^{dL} + \varepsilon_{\alpha\beta}^{dR}$. The effect of NSI with down-type quarks on the neutrino detection has been discussed at Ref. [1].

ANALYSIS OF SOLAR AND KAMLAND DATA

Here we reanalyse the robustness of the oscillation interpretation of the solar neutrino data in the presence of non–standard interactions. We perform a complete analysis of the most recent solar and KamLAND neutrino data using a numerical computation for the survival probabilities in the light as well as in the dark side of the mixing angle, for values of Δm^2 in the range of 10^{-6} to 10^{-3} eV^2 and running also the effective

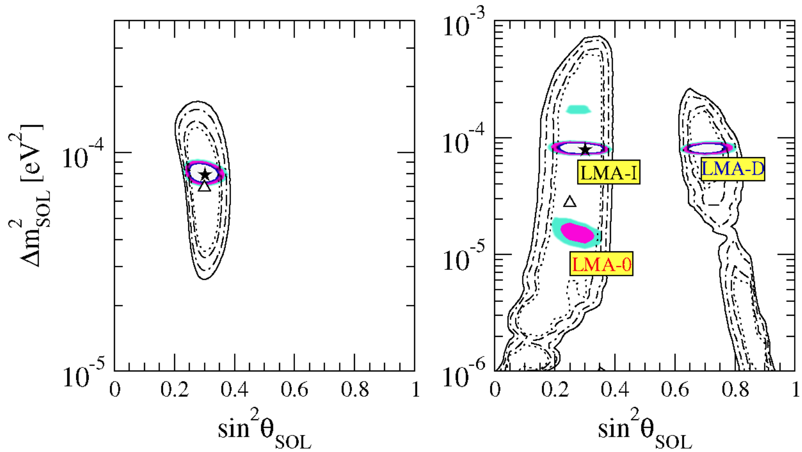

FIGURE 1. Left panel: 90%, 95%, 99% and 99.73% C.L. allowed regions of the neutrino oscillation parameters from the analysis of the latest solar data (hollow lines), and from the combined analysis of solar and KamLAND data (colored regions). Right panel: allowed regions for the generalized OSC + NSI case, corresponding to a solar only analysis (hollow lines) and to a combined solar+KamLAND analysis (colored regions).

TABLE 1. Best fit solar neutrino oscillation points with and without non-standard neutrino interactions.

	$\sin^2\theta_{SOL}$	Δm^2 [eV^2]	ε	ε'	χ^2
OSC analysis					
LMA-I	0.29	8.1×10^{-5}	–	–	79.9
OSC+NSI analysis					
LMA-I	0.30	7.9×10^{-5}	0	-0.05	79.7
LMA-D	0.70	7.9×10^{-5}	-0.15	0.90	80.2
LMA-0	0.25	1.6×10^{-5}	0.10	0.30	86.8

NSI couplings ε and ε' in the range $[-1,1]$[2]. Our results for the pure oscillation case ($\varepsilon = \varepsilon' = 0$) are shown in the left panel of Fig. 1. The best fit point for this global analysis is given by $\sin^2\theta_{SOL} = 0.29$ and $\Delta m^2 = 8.1\times10^{-5}$ eV ^{2}. This is in excellent agreement with the results obtained in [5] for the solar case. Concerning the generalized OSC+NSI picture, our results are shown in the right panel of Fig. 1 and Table 1. One sees that, in the light side, we obtain a region of allowed oscillation parameters larger than in the pure oscillation case, but more restricted than those obtained in previous

[2] More details about the statistical analysis performed can be found at Ref.[1]

OSC+NSI analysis of Refs. [14, 15] due to the effect of the recent KamLAND data, visible mainly in Δm^2. The table gives the parameter best fit values for the OSC and OSC+NSI fits. For the OSC+NSI analysis the best fit occurs for $\varepsilon = 0.0$ and $\varepsilon' = -0.05$. Clearly the quality of the fit obtained with and without NSI is comparable, as seen from the χ^2 values given in the last column of the table. The most remarkable result is, however, the appearance of an additional solution in the dark side region, LMA-D. This solution has $\sin^2\theta_{\rm SOL} = 0.70$ and the same Δm^2 value as the LMA-I solution and is significantly better than the LMA-0 OSC+NSI solution of Refs. [14, 15], as shown in the table. On the other hand, it is nearly degenerate with the LMA-I solution, as seen by the χ^2 value. This solution is characterized by $\varepsilon' = 0.90$, although lower values ~ 0.75 are allowed at 3σ. Even if embarrassingly large, one sees that such large NSI strength values are perfectly compatible with all existing solar and reactor neutrino data, including the small values of the neutrino masses indicated by current oscillation data. This opens a potentially physics challenge for upcoming low energy solar neutrino experiments, such as Borexino. Note that large NSI values could affect also solar neutrino detection, as considered in [16]. In what follows we give a discussion of the role of other experiments in probing neutrino properties at the level implied by the LMA-D solution.

CONSTRAINTS ON NSI: PRESENT AND FUTURE

As we just saw there are constraints on non-standard neutrino interaction strength parameters that follow from current solar and KamLAND data. The existence of NSI could also affect neutrino-nucleon scattering and there are laboratory data that potentially constrain their allowed strength. Moreover, one must check restrictions that follow from atmospheric data. Here we discuss their complementarity.

Solar and KamLAND

We can derive limits on NSI parameters from solar and KamLAND data by displaying our χ^2 as a function of the NSI parameters ε or ε' and marginalizing with respect to the remaining three parameters. Figure 2 gives the $\Delta\chi^2$ profiles with respect to ε and ε'. From here one can determine the corresponding constraints on ε and ε'. We can see that at 90% C.L. $-0.93 \leq \varepsilon \leq 0.30$ while for ε' the only forbidden region is $[0.20, 0.78]$. The dashed lines in Fig. 2 denote the ultimate reach of this method of constraining NSI parameters (through their effect in solar neutrino propagation), namely they correspond to the case where solar neutrino oscillation parameters Δm^2 and $\theta_{\rm SOL}$ are determined with infinite precision. One sees that in this ideal case the allowed range narrows down mainly for negative NSI parameter values. We conclude that there is substantial room still left for sub–leading non-standard neutrinos conversions in matter and, moreover, that the determination of solar neutrino oscillation parameters, especially the solar mixing angle, is currently ambiguous. It is unlikely that more precise reactor measurements by KamLAND will resolve this mixing angle ambiguity, as they are expected to constrain mainly Δm^2.

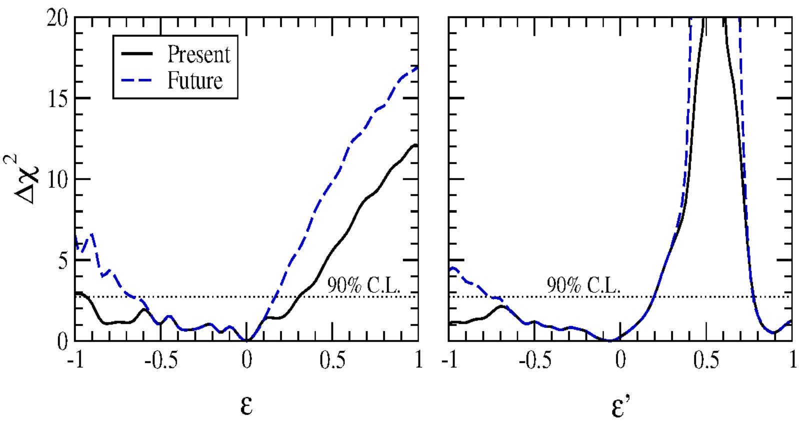

FIGURE 2. Constraining NSI parameters with solar and KamLAND neutrino data: dependence of $\Delta\chi^2$ with respect to ε and ε', illustrating the current limits.

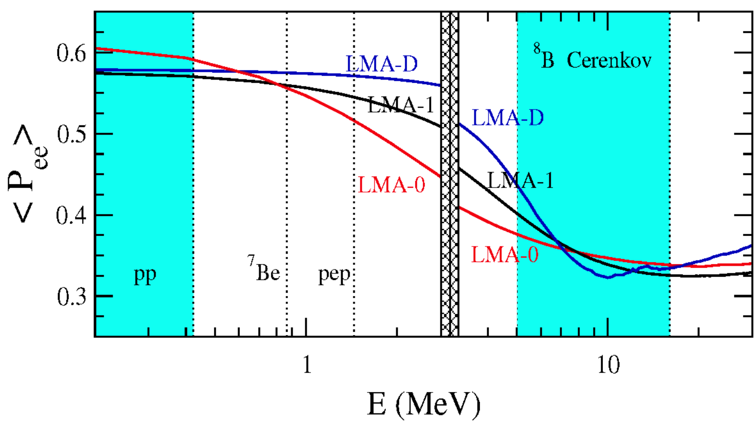

FIGURE 3. Predicted neutrino survival probability for low-energy neutrinos (left) and boron neutrinos (right) at the best fit points of the LMA-I, LMA-D and LMA-0 solutions.

In Fig. 3 we present the predicted neutrino survival probabilities versus energy, from the region of pp neutrinos up to the high energy solar neutrinos, for the three best–fit points of the allowed regions found above. One sees that the solutions predict different rates for the low energy neutrinos, so that future low energy solar neutrino experiments may have a hope of disentangling these solutions. Similarly, in the region of boron neutrinos our LMA-D solution also predicts a distortion in the spectrum that might be detectable at future water Cerenkov experiments such as UNO or Hyper-K [17], given the high statistics expected.

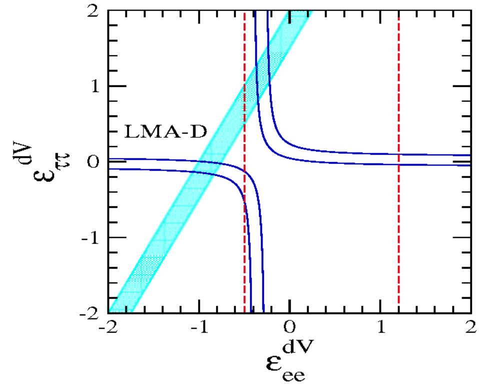

FIGURE 4. Consistency between the ε' coupling required for our LMA-D solution (shaded band) and the regions allowed by atmospheric data in the analytic approximation of Ref. [19] for $\varepsilon^{dV}_{e\tau} = 0.21$ (solid lines). The laboratory constraints are also shown (dashed lines).

Laboratory experiments

The laboratory bounds on the neutrino non-standard interactions with down-type quarks can be summarized as $|\varepsilon^{dP}_{\tau e}| < 0.5$, $|\varepsilon^{dR}_{\tau\tau}| < 6$, $|\varepsilon^{dL}_{\tau\tau}| < 1.1$, $-0.6 < \varepsilon^{dR}_{ee} < 0.5$, $-0.3 < \varepsilon^{dL}_{ee} < 0.3$, $0.6 < \varepsilon^{dL}_{ee} < 1.1$, see e. g. Ref [11]. Here we are interested in vector-like NSI couplings. For the case of ε^{dV}_{ee}, these bounds can be translated to $-0.5 < \varepsilon^{dV}_{ee} < 1.2$, while for $\varepsilon^{dV}_{\tau\tau}$ one finds a much wider range. However, we stress that these bounds have been obtained assuming that only one parameter is effective at a time. Relaxing this assumption opens more freedom. Assuming maximal mixing in the 2–3 sector in Eq. (4), one has

$$\varepsilon = -0.15 \quad \rightarrow \quad \varepsilon^{dV}_{e\tau} = 0.21 \tag{5}$$

$$\varepsilon' = \quad 0.90 \quad \rightarrow \quad \varepsilon^{dV}_{\tau\tau} = 2\,(\varepsilon^{dV}_{ee} + 0.90) \tag{6}$$

From this one can see explicitly that, even taking the above constraints at face value, they still leave room for our degenerate dark-side solution with $\varepsilon' = 0.90$.

Atmospheric data

Concerning the atmospheric neutrino data, it is known that a large NSI strengths can originate a suppression of the neutrino oscillation amplitude. This has indeed been used in a two-neutrino analysis [18] in order to obtain relatively strong bounds on the NSI strength. However, in a 3–neutrino analysis of atmospheric data [19] it has been explicitly shown that large NSI strengths are not excluded. In particular, these authors have found two specific scenarios where somewhat large NSI strengths can fit well the experimental data, because their effect will be indistinguishable from the standard oscillation case, at least at high and low energies. Adapting their definitions to our notation, and using their analytical description, we obtain the two branches indicated in Fig. 4. One sees that the shaded band corresponding to our LMA-D solution at 90% C.L. (with $\varepsilon_{e\tau}^{dV} = 0.21$) intersects these branches in two disjoint regions, suggesting that, indeed, the NSI couplings required by the LMA-D solution are compatible with the atmospheric neutrino data. However, in a more complete numerical analysis of atmospheric neutrino data [20], it has been shown that values of $\varepsilon_{\tau\tau}^{dV}$ in the right region are not allowed by atmospheric data: only the left disjoint region is compatible with atmospheric neutrino data. As indicated by the dashed lines in Fig. 4 one can see that ε_{ee}^{dV} values in this region lie outside the range allowed by current laboratory data. This leads us to conclude that the LMA-D solution induced by the simplest non-standard interactions of neutrinos with only down-type quarks is ruled out by its incompatibility with atmospheric and laboratory data. However, one can verify that for the general case where neutrinos have other NSI couplings one can reconcile the above laboratory bounds with the parameters required by the LMA-D solution.

CONCLUSIONS

We have reanalysed the status of the LMA oscillation interpretation of the solar neutrino data in a more general framework where non-standard neutrino interactions are present. We have seen that combining the solar neutrino data, including the latest SNO fluxes of the salt phase with the full KamLAND data sample still leaves room for a degenerate determination of solar neutrino oscillation parameters. To this extent the solar neutrino oscillation parameters extracted from the experiments may be regarded as non-robust. In addition to the lower LMA-0 solution, we have found a LMA-D solution characterized by values of the solar mixing angle larger than $\pi/4$. This solution requires large non-universal neutrino interactions on down-type quarks. While the LMA-0 solution is already disfavored, and will soon be in conflict with further data, e.g. future KamLAND reactor data, the degeneracy implied by LMA-D solution will not be resolved by more precise KamLAND reactor measurements. This shows that the determination of solar neutrino parameters only from solar and KamLAND data is not fully robust. It is crucial to consider other data samples, such as atmospheric and laboratory data, since these bring complementary information. In the present case they allow one to rule out the LMA-D solution induced by the simplest NSI between neutrinos and down-type-quarks-only, given the large values of the non–universal NSI couplings required by that solution. It is therefore important to perform similar analyses for the more general case of non-standard interactions involving electrons and/or up-type quarks. Only in such scenario (NSI with u-type, d-type and electrons) we can confidently establish the robustness of the oscillation interpretation. Further experiments, like low-energy solar neutrino experiments are therefore required in order to clear up the situation.

ACKNOWLEDGMENTS

Work supported by the European Commission under the RTN contract MRTN-CT-2004-503369.

REFERENCES

1. O. G. Miranda, M. A. Tortola and J. W. F. Valle, JHEP **0610**, 008 (2006) [hep-ph/0406280].
2. K. Eguchi *et al.*, [KamLAND Collaboration], Phys. Rev. Lett. **90**, 021802 (2003) [hep-ex/0212021].
3. T. Araki *et al.*, [KamLAND Collaboration], Phys. Rev. Lett. **94**, 081801 (2005) [hep-ex/0406035].
4. For a review of solar neutrino experiments see A. B. McDonald, New J. Phys. **6**, 121 (2004) [astro-ph/0406253] and references therein. For the latest atmospheric, K2K and MINOS neutrino oscillation results see H. Gallagher, Nucl. Phys. B Proc. Suppl. **143**, 79 (2005); M. H. Ahn *et al.*, Phys. Rev. D **74**, 072003 (2006) [hep-ex/0606032] and D. G. Michael *et al.*, [MINOS Collaboration], Phys. Rev. Lett. **97**, 191801 (2006) [hep-ex/0607088].
5. M. Maltoni, T. Schwetz, M. A. Tortola and J. W. F. Valle, New J. Phys. **6**, 122 (2004) [hep-ph/0405172 v5].
6. J. Schechter and J. W. F. Valle, Phys. Rev. D **24**, 1883 (1981), Err. Phys. Rev. D **25**, 283 (1982).
7. E. K. Akhmedov, Phys. Lett. B **213**, 64 (1988); C. S. Lim and W. J. Marciano, Phys. Rev. D **37**, 1368 (1988).
8. L. Wolfenstein, Phys. Rev. D **17** 2369 (1978); J. W. F. Valle, Phys. Lett. B **199** 432 (1987).
9. J. W. F. Valle, Prog. Part. Nucl. Phys. **26**, 91 (1991).
10. G. Mangano *et al.*, Nucl. Phys. B **756**, 100 (2006) [hep-ph/0607267]; A. de Gouvea and J. Jenkins, Phys. Rev. D **74** 033004 (2006) [hep-ph/0603036]; J. Barranco, O. G. Miranda, C. A. Moura and J. W. F. Valle, Phys. Rev. D **73** 113001 (2006) [hep-ph/0512195].
11. S. Davidson, C. Pena-Garay, N. Rius and A. Santamaria, JHEP **0303** 011 (2003) [hep-ph/0302093].
12. Z. Berezhiani and A. Rossi, Phys. Lett. B **535** 207 (2002) [hep-ph/0111137].
13. M. Apollonio *et al.*, [CHOOZ Collaboration], Phys. Lett. B **466**, 415 (1999) [hep-ex/9907037].
14. A. Friedland, C. Lunardini and C. Pena-Garay, Phys. Lett. B **594**, 347 (2004) [hep-ph/0402266].
15. M. M. Guzzo, P. C. de Holanda and O. L. G. Peres, Phys. Lett. B **591**, 1 (2004) [hep-ph/0403134].
16. Z. Berezhiani, R. S. Raghavan and A. Rossi, Nucl. Phys. B **638**, 62 (2002) [hep-ph/0111138].
17. UNO collaboration Homepage: http://superk.physics.sunysb.edu/nngroup/uno/main.html.
18. N. Fornengo, M. Maltoni, R. T. Bayo and J. W. F. Valle, Phys. Rev. D **65** (2002) 013010.
19. A. Friedland, C. Lunardini and M. Maltoni, Phys. Rev. D **70**, 111301 (2004) [hep-ph/0408264].
20. A. Friedland and C. Lunardini, Phys. Rev. D **72** (2005) 053009 [hep-ph/0506143].